NIH Public Access
Author Manuscript
Langmuir. Author manuscript; available in PMC 2011 April 20.

Published in final edited form as:
Langmuir. 2010 April 20; 26(8): 5848–5855. doi:10.1021/la903770s.

More Fluorous Surface Modifier Makes it Less Oleophobic: Fluorinated-Siloxane Copolymer/PDMS Coatings

Wei Zhang[1], **Ying Zheng**[1], **Lorenzo Orsini**[1], **Andrea Morelli**[2], **Giancarlo Galli**[2], **Emo Chiellini**[2], **Everett E. Carpenter**[3], and **Kenneth J. Wynne**[1,*]

[1]Department of Chemical and Life Science Engineering, Virginia Commonwealth University, 601 West Main St., Richmond, VA 23284-3028

[2]Dipartimento di Chimica e Chimica Industriale, Università di Pisa, UdR Pisa – INSTM, Via Risorgimento 35, 56126 Pisa, Italy

[3]Department of Chemistry, 1001 West Main St., Richmond, Virginia 23284-2006

Abstract

A copolyacrylate with semifluorinated and polydimethylsiloxane side chains (D5-3) was used as a surface modifier for a condensation cured PDMS coating. The decyl fluorous group is represented by “D”; “5” is a 5 kDa silicone, and “3” the mole ratio of fluorous to silicone side chain. Wetting behavior was assessed by dynamic contact angle (DCA) analysis using isopropanol, which differentiates silicone and fluorous wetting behavior. Interestingly, a maximum in surface oleophobicity was found at low D5-3 concentration (0.4 wt%). Higher concentrations result in decreased oleophobicity reflected in decreased contact angles. To understand this unexpected observation, dynamic light scattering (DLS) studies were initiated on a model system consisting of hydroxyl-terminated PDMS (18 kDa) containing varying amounts of D5-3. DLS revealed D5-3 aggregation as a function of temperature and concentration. A model is proposed by which D5-3 surface concentration is depleted via phase separation favoring D5-3 aggregation at concentrations >0.4 wt%, that is, the CMC. This model suggests increasing aggregate / micelle concentrations at increased D5-3 concentration. Bulk morphologies studied by scanning electron microscopy (SEM) and atomic force microscopy (AFM) support this model by showing increased aggregate concentrations with increased D5-3 >0.4 wt%.

Keywords

PDMS; surface modification; silicone; semifluorinated; oleophobicity; CMC; aggregation; contact angle; surface tension; fluorous/PDMS copolyacrylate

Introduction

The solubility parameter of poly(dimethylsiloxane) (PDMS, $\delta = 7.3$ $(cal/cm^3)^{1/2}$)[1] is similar to organic liquids such as hexane ($\delta = 7.2$ $(cal/cm^3)^{1/2}$) and consequently silicones are swollen by many organic solvents. Resistance to organic solvents is important in applications such as microfluidic devices[1] and fuel resistant tubing and gaskets. For these applications, introducing fluorocarbon [$R_f(CH_2)_n$] groups into PDMS as side chains reduces swelling. For example, poly

*To whom correspondence should be addressed. Chemical and Life Science Engineering, Virginia Commonwealth University, 601 W. Main Street, Richmond, VA 23284-3028, Ph: 804-828-9303, Fax:804-828-3846, kjwynne@vcu.edu.

Supporting Information Available. These materials are available free of charge via the Internet at http://pubs.acs.org.

NIH-PA Author Manuscript
NIH-PA Author Manuscript
NIH-PA Author Manuscript

NIH-PA Author Manuscript

NIH-PA Author Manuscript

NIH-PA Author Manuscript

(trifluoropropyl methyl siloxane), (-Si($CH_2CH_2CF_3$)(CH_3)-O-)$_n$ has increased oleophobicity with a surface tension of 13.6 mJ/m^2.[2] Introducing longer fluorocarbon side-chains results in lower surface tensions.[3] A surface tension of 9.5 mJ/m^2 was achieved for poly (methylnonafluorohexylsiloxane) surface.[4] Perfluoropolyether functionalized siloxanes are alternatives to fluoroalkyl side chains and have particularly low surface free-energy (8 mJ/m^2).[5] Perfluoropolyether / PDMS copolymers have improved oleophobicity for applications such as microfluidics.[6,7]

Using a semifluorinated trialkoxysilane for condensation cure results in formation of a fluorous siliceous domain and improves oleophobicity through the formation of a $R_fSiO_{1.5}$ domain,[8] but the surface is mechanically fragile.[9] Block copolymers with semifluorinated and silicone segments were used to increase oleophobicity of PDMS.[10] The latter work demonstrated that wetting behavior using isopropanol distinguished between a fluorous and silicone surface.

Surface modification employed by our group[10] and others[11,12] is generally based on the assumption that increasing the semifluorinated component concentration improves oleophobicity. Herein, we report a result that is a departure from this notion. Using copolymer **1** as a surface modifier for condensation cured PDMS and isopropanol as a probe liquid,[10] a maximum in surface oleophobicity, is found at a low concentration (~0.4 wt%). To understand this unexpected observation, dynamic light scattering (DLS) was used on a model system consisting of polydimethylsiloxane as a solvent and polymer **1** as a solute. A model is proposed that correlates variations in surface oleophobicity with the critical micelle concentration for the formation of aggregates observed by DLS for the model system and by SEM and AFM on coatings.

NIH-PA Author Manuscript
NIH-PA Author Manuscript
NIH-PA Author Manuscript

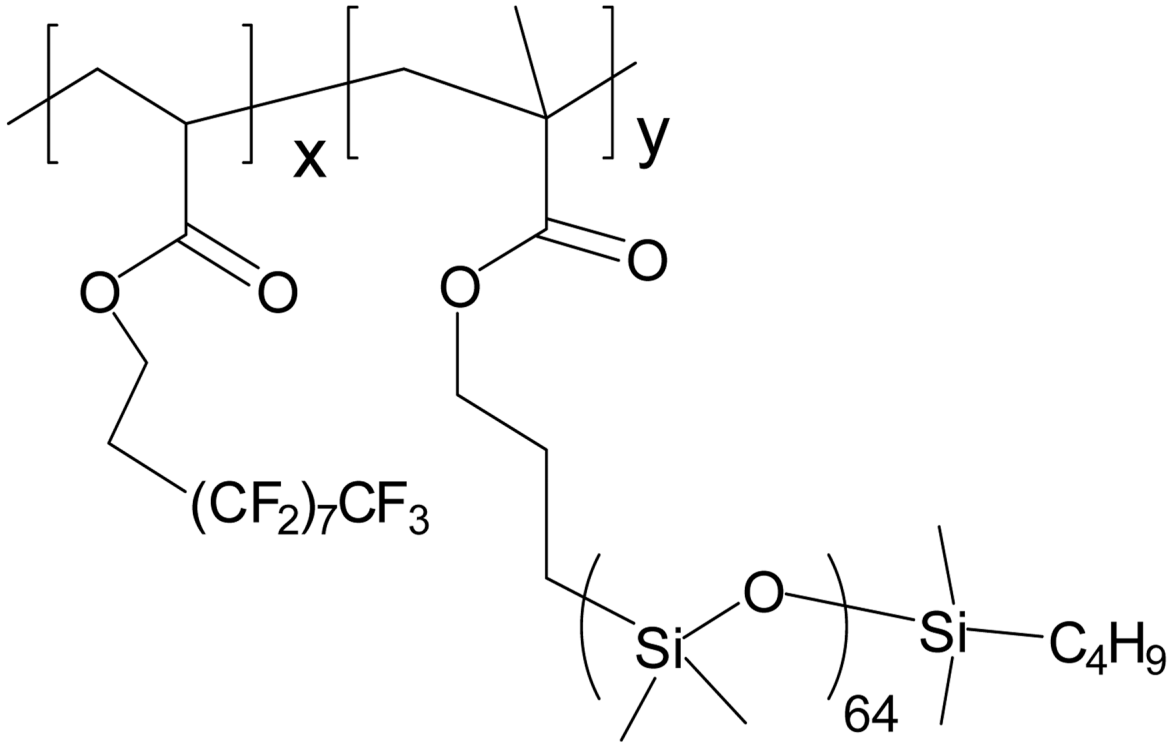

1

Experimental Section

Materials

1H,1H,2H,2H-perfluorodecyl acrylate (AF8) was purchased from Fluorochem and used as received. Monomethacryloyloxypropyl-terminated polydimethylsiloxane (MCR-M17) was purchased from ABCR and used as received. Polydimethylsiloxane (M_w = 26kDa, DMS-S31), PDMS (M_w = 18kDa) (DMS-S27) and polydiethoxysiloxane (PDES) with the empirical formula $[(CH_3CH_2O)_2SiO]_n$ were purchased from Gelest and used as received. PDES is a condensation cure (solgel) crosslinker and siliceous domain precursor sometimes called ES40. 2,2′-Azo-bis-isobutyrylnitrile (AIBN), trifluorotoluene (TFT), dibutyltin diacetate (DBTDA) were purchased from Sigma-Aldrich and used as received. Isopropanol (HPLC grade, 99.9%) for dynamic contact angles measurements was also purchased from Sigma-Aldrich.

D5-3 synthesis and characterization

The fluorous / PDMS modifier D5-3 was prepared, purified, and characterized as described in a previous procedure.[13] ^{1}H NMR ($CDCl_3$): δ(ppm): 0.1 ($SiCH_3$), 0.5 ($SiCH_2$), 0.9–3.0 ($SiCH_2(C\underline{H}_2)_2C\underline{H}_3$, CH_2CHCCH_3, $COOCH_2C\underline{H}_2CH_2Si$, CH_2CF_2), 4.0 ($COOC\underline{H}_2(CH_2)_2Si$), 4.5 ($COOC\underline{H}_2CH_2CF_2$). ^{19}F NMR ($CDCl_3$/$CF_3COOH$): δ (ppm): −6 ($CF_3$), −38 ($CH_2CF_2$), −47 to −49 ($CF_2$), −51 ($CF_2CF_3$). The copolymer composition was calculated from the integrated areas of the ^{1}H NMR signals at 4.5 ppm and 4.0 ppm attributed to the $COOCH_2$ groups of the fluorinated and siloxane units, respectively.

NIH-PA Author Manuscript

NIH-PA Author Manuscript

NIH-PA Author Manuscript

Differential scanning calorimetry (DSC) measurements were performed on a TA instrument Q1000. Samples (5–15 mg) were used with 10 °C/min heating and cooling rates. Temperature and energy calibrations were carried out using standard samples of tin, indium and zinc. The maximum in the relevant enthalpic peak was taken as the phase transition temperature.

Blends and coating preparation

All coating compositions employed PDMS (M_w = 26 kDa), 5 g; PDES, 0.125 g, 2.5 wt%; DBTDA, 25 mg, 0.5 wt%. D5-3 modifier was varied as follows (wt%, mg): 0 (0), 0.1 (5), 0.2 (10), 0.3 (15), 0.4 (20), 0.6 (30), 0.8 (40), 1.2 (60), 2 (100), 3.5 (185), 5 (250). Polymer blends were prepared by mixing copolymer **1** and PDMS with a magnetic stirrer under an infrared lamp until an optically transparent solution resulted. The reaction mixture temperature was approximately 60 °C. The viscosity increased and the mixture was removed from the heat source. Coatings were prepared by dip coating onto glass cover slips under ambient conditions. The coated slides were returned to the area under the heat lamps for up to 4 hr. Cure was completed at 100 °C overnight. Cured coatings were stored at room temperature. Samples for SEM measurements were cured in aluminum pans at selected temperatures for at least 24 hours.

Dynamic contact angle (DCA) experiments were carried out by a Wilhelmy plate method using a Cahn model 312 contact angle analyzer. Isopropanol was used for all samples with an immersion/withdrawal rate of 100 μm/s and a dwell time between immersion and withdrawal of 8 s. Reported contact angles are averages of several determinations. Accuracy is generally ± 1–2°.

Dynamic light scattering (DLS) measurements were performed using a Malvern Instruments Zetasizer Nano-ZS instrument (Malvern Instruments Ltd., United Kingdom). Scattered light at 173° is measured and used to calculate the particle sizes. Samples were prepared by mixing copolymer **1** with PDMS (M_w = 18,000, viscosity = 800 cSt at 25 °C) with a magnetic stirrer at 60 °C for 48 h. While still warm, the solution was filtered with a 0.2μm PTFE syringe filter. The PDMS room temperature viscosity (800 cSt) was used for convenience during DLS measurements. A temperature correction was employed for data analysis. For each run, 10–20 measurements were taken and mean particle sizes are listed in Table 1. Additional information concerning the experimental method may be found in Supplemental Information.

Scanning electron microscopy (SEM)

Condensation-cured samples were fractured and mounted on 10 mm aluminum stubs. Samples were sputter coated using a gold target for 120 seconds in an EMS 550x sputter coater (Hatfield, PA, USA). The fractured surface was viewed by tilting the sample holder 90 degrees. The microscope was operated at 15 keV under high vacuum using a Zeiss EVO 50 XVP scanning electron microscope (Peabody MA, USA).

Tapping Mode Atomic Force Microscopy (TM-AFM)

A Dimension Nanoscope V (Veeco, CA) atomic force microscope was used for morphological analysis of fracture surfaces. Runs were performed in tapping mode using silicon crystal cantilevers (40 N/m). The tapping force was increased from soft to hard by decreasing the setpoint ratio r_{sp} or A_{exp}/A_o, where A_o is free oscillation amplitude and A_{exp} is the experimental oscillation amplitude.

Results and Discussion

Polymer surface modifier 1, (D5-3)

The synthesis and structure of copolyacrylate **1** having semifluorinated and silicone side chains has been previously described.[13] The polydimethylsiloxane side chain have a molecular weight

NIH-PA Author Manuscript

NIH-PA Author Manuscript

NIH-PA Author Manuscript

of 5×10^3 g/mol. This surface modifier is designated D5-3, where: "D" represents the decyl fluoroalkyl group; "5" the 5 kDa silicone, and "3" the ratio of moles of fluorinated side chain to silicone side chain (x/y).

D5-3 is a colorless waxy solid. Thermal transitions for D5-3 were analyzed by modulated DSC. As shown in Figure 1 T, the total heat flow reveals two melting transitions between −80 and 60 °C. The endotherm at −55 °C is due to PDMS melting.[14] The endotherms at 36 °C and 42 °C are assigned to melting transitions associated with an ordered semifluorinated side chain phase. These endotherms do not appear as reversible contributions to heat flow. This observation is ascribed to slow kinetics for formation of the ordered fluorous phases and the low enthalpy associated with the transitions.

PDMS and D5-3 modified PDMS coatings

Coatings were prepared by condensation cure according to a variation of a reported method.[13] Hydroxyl terminated PDMS, polydiethoxysiloxane (crosslinker / siliceous domain precursor) and dibutyltin diacetate catalyst were mixed manually. Initial attempts to prepare D5-3 modified coatings at ambient temperature (21–23 °C) resulted in hazy solutions and translucent coatings (Figure 2A–B). Optically transparent solutions and coatings were obtained by mixing under an infrared lamp (Figure 2C–D). The reaction mixture temperature under these conditions was about 60 °C. The reaction mixture was removed from the heat source for dip coating glass slides. Coated slides were placed under the infrared lamp for the initial stage of cure. Subsequently, condensation cure was completed at 100 °C.

DCA analysis of wetting behavior

Previously, we showed that isopropanol perfectly wets condensation cured PDMS ($\theta_{adv} = \theta_{rec} = 0°$).[10] In contrast, θ_{adv} for styrene-siloxane block copolymer **2** (BSF8), θ_{adv} was greater than 60°. Thus, isopropanol wetting behavior differentiates between PDMS and fluorous surfaces. Herein, Dynamic Contact Angle (DCA) wetting behavior for neat D5-3 and D5-3 modified PDMS was investigated using isopropanol contact angles as metrics for the degree of surface modification.

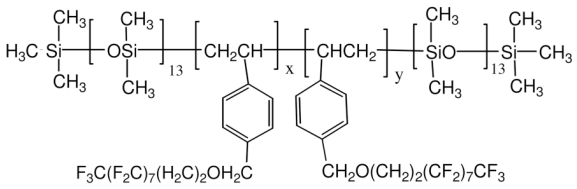

2 (x + y = 112)

Isopropanol—The isopropanol wetting behavior for D5-3 dip coated onto a glass cover slip serves as a reference point. Figure 3A shows DCA force distance curves (fdc's) for isopropanol/D5-3. There is a modest attenuation in θ_{adv} from 89 to 85° over four cycles; θ_{rec} remains constant at 33°. These results may be compared to the static contact angle of 59° reported earlier.[13] The corresponding values for isopropanol/BSF8 are $\theta_{adv}/\theta_{rec} = 64°/44°$. Comparing the DCA results shows that D5-3 is more resistant to initial wetting, but surface reorganization results in a lower value for θ_{rec} compared to BSF8.

The ability of D5-3 to modify condensation cured PDMS was investigated. Figure 4A shows θ_{adv} (isopropanol) as a function of wt % D5-3 for condensation cured silicone coatings prepared as described above. A sharp increase in oleophobicity (θ_{adv}, ≥ 90°) is observed up to 0.4 wt% D5-3. The maximum θ_{adv} for isopropanol is similar to that for neat D5-3 (Figure 3A) as is the maximum for θ_{rec} (~ 35°) (Figure 3B). Above this concentration θ_{adv} *decreases* leveling off

NIH-PA Author Manuscript

NIH-PA Author Manuscript

NIH-PA Author Manuscript

to 50 ± 5° between 1–5 wt%. To confirm the unusual maximum at 0.4 wt% D5-3, DCA measurements at 0.1, 0.4, and 2.0 wt% D5-3 were repeated with a new batch of materials; DCA fdc's are in Figures S1-A (0.1), S1-B (2.0), and Figure 3B (0.4). First cycle θ_{adv} for these measurements are represented by Δ in Figure 4A; these repeat determinations reproduce prior data and verify the existence of the 0.4 wt% maximum.

The contrasting isopropanol wetting behavior for 0.4 and 2.0 wt% D5-3 is characteristic of "more is less". DCA fdc's for 0.4 and 2 wt% D5-3/PDMS are shown in Figure 3B and 3C, respectively. Two features of isopropanol wetting behavior for 0.4 wt% D5-3/PDMS are noteworthy. The first advancing fdc is unique and yields $\theta_{adv} = 94°$. The subsequent emersions ($\theta_{rec} = 29°$) and immersions ($\theta_{adv} = 84°$) have identical fdc's. Careful inspection of Figure 4A shows that the apparent scatter of data points in the vicinity of 0.4 wt% is due to the inclusion of all fdc cycles. The striking decrease in θ_{adv} above 1 wt% D5-3 (Figure 4) is typified by DCA fdc's for 2 wt% D5-3/PDMS shown in Figure 3C. θ_{adv} drops by 40° to 46° for 2 wt% D5-3/PDMS and θ_{rec} decreases by 7° to 23°.

Wetting behavior for 0.4 wt% D5-3/PDMS bears close resemblance to the neat modifier (Figure 3A. Even with the 10° drop after the first fdc, the isopropanol θ_{adv} of 84° for 0.4 wt% D5-3/PDMS is higher than previously reported for neat isopropanol/BSF8 ($\theta_{adv} = 64°$).[10] Like neat D5-3, θ_{rec} (29°) for 0.4 wt% D5-3 is lower than that for BSF8 (44°). For 0.4 wt% D5-3/PDMS, the reduction of θ_{adv} from 94° for the first fdc to a constant value of 84° is attributed to a localized surface reorganization or weak isopropanol chemisorption, as the higher θ_{adv} is restored after the coating is briefly dried and re-tested.

Water—In contrast to the dependence of isopropanol wetting on D5-3 concentration, corresponding DCA analysis using water showed more subtle changes (Figures S2–S5). Figure S3 shows fdc's for the neat D5-3 modifier coating that yield $\theta_{adv}/\theta_{rec}$ of 128 / 78°. These values are close to those observed for 2 wt% D5-3/PDMS coating (Figure S4). Furthermore, the large contact angle hysteresis, $\Delta_\theta = 50°$, argues for a fluorous compared to a PDMS-like surface. As a reference, DCA fdc's for condensation cured PDMS shows $\theta_{adv}/\theta_{rec}$ of 119 / 97° (Figure S5).

In a study of contact angles versus D5-3 concentration, there is scatter (115 – 130°) in θ_{adv} and θ_{rec} values below 1 wt% D5-3 (Figure S2). Consistent data are only acquired above 2 wt% D5-3. A trend of decreasing θ_{adv} for successive cycles: 1 > 2 > 3 is observed, while θ_{rec} values for successive cycles are in the order: 1 < 2 < 3. This trend is pronounced for 0.5 – 1 wt% D5-3 concentrations giving rise to increases up to 20°in θ_{rec}.

Despite the complex cycle-dependent DCA contact angle data for water, one unexpected result emerged, namely D5-3 modification blocked PDMS contamination of water during the DCA analysis. We have previously shown that intrinsic $\theta_{adv}/\theta_{rec}$ values for PDMS are only obtained by using a large surface area that precludes oil buildup on the water surface.[15] Water contamination, which reduces water surface tension, results in a discontinuous change in $\theta_{adv}/\theta_{rec}$ values after DCA cycle 1 (119/97°) to 109/103° for cycle 3 (Figure S5). Interestingly, over the course of three cycles, which is a total of about 10 min immersion, no detectable water contamination occurs for D5-3 modified PDMS (Figure S4). Because permeability is a function of solubility and diffusivity, the insolubility of PDMS oils in the surface modifier greatly attenuates diffusion from the bulk PDMS coating.

For isopropanol wetting, the remarkable 95° maximum in θ_{adv} at ~0.4 wt% followed by a drop to ~50° at concentrations greater than 1 wt% (Figure 4) suggested a phase transition might be responsible for a decrease in surface concentration of fluorous groups. The difficulty in achieving miscibility for D5-3 in the PDMS resin reinforced this notion. D5-3 is an amphiphile in PDMS as the immiscibility of fluorocarbons in silicone fluids is well established.[1] While a

NIH-PA Author Manuscript

NIH-PA Author Manuscript

NIH-PA Author Manuscript

large body of information is available on solubility and aggregation of amphiphiles in water,[16] comparable information does not exist for fluorous-silicone amphiphiles. To acquire fundamental knowledge on phase behavior, dynamic light scattering was carried out on a model system.

DLS measurements

DLS measurements were taken using a similar molecular weight PDMS fluid (M_w = 18 kDa) as solvent. By varying D5-3 concentration (0.1 – 5.0 wt%), micelle formation/aggregation was estimated at 10 to 60 °C. Data analysis is described in the Supplemental Information.

Figure 5 illustrates representative DLS data for 3 wt% D5-3 in PDMS at 20 °C. Figure 5 A shows the correlation function (data points) and cumulant analysis (solid line fit) using the "multiple narrow size distribution" setting (details in Supplemental Information). Particle diameter histograms for this determination are in Figure 5 B. The DLS contribution from particles centered at 75 nm is dominant. When the D5-3 concentration was ≤ 0.3 wt%, aggregates in this size distribution range were not detected, while at ≥ 0.5 wt%, aggregates were clearly observed (Table 1). The dependence of calculated particle size on temperature for each concentration is shown in Table 1.

Low intensity peaks at 3 nm are also observed (Figure 5 B). Such low intensity peaks were often seen at 1–15 nm below the phase boundary (vide infra). The intermittent observation of 1–15 nm aggregates may be a consequence of non-equilibrium conditions. Below the phase boundary, small fragments may not have had time to aggregate.

Above the phase boundary, low intensity peaks for small aggregates are always observed irrespective of DLS data analysis mode (Table 1). These 8–15 nm aggregates may be remnants of larger particles that have not fully dissolved. The high viscosity of the 18 kDa PDMS solvent likely militates against rapid dissolution. Whatever their origin, the small particles are kinetically stable over the time of DLS measurements.

Figure 6 shows a plot of DLS data vs. temperature (Table 1) for 5 wt% D5-3. On cooling from 60 to 25 °C, the mean particle size was invariant (~12 nm) until 41 °C, at which point a sudden increase occurs. By fitting straight lines through data above and below 40 °C the intercept identifies the transition point for aggregate formation. Applying the same analysis to the other concentrations, a phase diagram of transition point dependence on D5-3 concentration is generated (Figure 7). Temperature dependent aggregate formation was detected for D5-3 concentrations from 0.5 – 5 wt%. The formation of aggregates with decreasing temperature is a UCST (upper critical solution temperature) type phase behavior. Lower weight percents are associated with lower temperatures for aggregate formation. Considering the relatively low concentrations that result in phase separation, the amphiphilic nature of D5-3, and analogous aggregation phenomena in aqueous solutions,[16] for the remainder of the results and discussion we use critical micelle concentration (CMC) to describe aggregation.

Micelle aggregation model

The mutual insolubility of silicones and fluorinated species[1] accounts for self association of C8 semifluorinated side chains that form ordered domains.[17,18] The tendency toward self-association is evidenced by DSC thermograms for D5-3 (Figure 1) that show endotherms at 36 and 42 °C attributed to melting or order-disorder transitions for self organized fluorous phases.[13] With increasing concentration, the temperature for the phase boundary reaches 40 °C at 5 wt%, suggesting a similar molecular origin for association of fluorous groups in PDMS solution and neat D5-3.

NIH-PA Author Manuscript

NIH-PA Author Manuscript

NIH-PA Author Manuscript

The PDMS matrix polymer comprises 92 to 97 wt% for the elastomeric coatings. With regard to D5-3 surface modification and aggregation, the presence of the siliceous phase from PDES sol gel chemistry (about 3 wt%) may be neglected. In contrast to the model D5-3 / silicone solutions, condensation cure via sol-gel reactions creates dynamic conditions due to initial reaction at ~60 °C, cooling to near ambient temperature for dip coating, and completion of condensation cure at 60 – 100 °C.

Based on the phase diagram for D5-3 in PDMS (Figure 7) and the contact angle dependence on D5-3 concentration (Figure 4), a model for D5-3 aggregation in the coating process is proposed in Figures 8. The first step involves self-aggregation via intramolecular association of fluorous and silicone side chains. The bicolor trapezoid provides a two dimensional representation of the initial aggregation of fluorous side chains. Dynamic light scattering for D5-3 solutions in PDMS suggests negligible intermolecular aggregation in dilute solution (Table 1). Thus, D5-3 is miscible at low concentrations in the coating reaction mixture below the CMC. As for conventional surfactants, the surface tension decreases with increasing concentration.[19–21] This is reflected in the rapid rise in θ_{adv} with increased D5-3 concentration, which is depicted in Figure 8 A–B.

As shown by the DLS data (Figure 7), D5-3 and PDMS form a one phase system at 60 °C. Reaction solutions are optically transparent at this temperature. Condensation polymerization at 60 °C is more rapid than at ambient temperature and viscosity increases over a few minutes. When the mixture is removed from the heat source for dip coating a substrate at 25 – 30 °C, despite increased viscosity, D5-3 aggregation occurs when the temperature of the uncured coating mixture crosses into the two phase region described by the phase diagram in Figure 7. The cold glass slide and the thinness of the coating contribute to heat transfer and cooling, which result in phase separation.

The next step in the coating process was placing the coated slides under the infrared lamp heat source for a few hours to affect initial cure. From SEM and TM-AFM imaging described below, re-dissolution of D5-3 is restricted due to continually increasing viscosity. Despite the increased temperature after replacement of the coated slide under the heat lamp at 60 °C, a non-equilibrium state determined by the phase diagram at 25–30 °C is “frozen in”.

With the phase diagram for D5-3 in PDMS and SEM and TM-AFM images described in the next sections, the model in Figure 8 explains isopropanol wetting as a function of D5-3 concentration. At increasing concentrations below the CMC, the surface concentration of D5-3 builds up and accounts for the rapid increase in θ_{adv} to > 90° (Figure 4). The model for this concentration range is depicted in Figure 8A. The 0.4 wt% concentration for maximum θ_{adv} (~95°) corresponds to the CMC at 24 °C and the depiction in Figure 8B. Higher D5-3 concentrations have higher temperatures for the onset of formation of a two phase system (Figure 7). Thus, during the initial stage of cure, D5-3 is soluble in the reaction mixture, but after cooling to 25–30 °C for dip coating, the surface concentration of D5-3 is controlled by the formation of two phases as described by the D5-3 / PDMS phase diagram. As noted earlier, phase separation may be regarded as a CMC or as UCST behavior. In any event, aggregates form as described by Figure 8C.

Above the CMC (Figure 8C) the surface is depleted of D5-3 due to the preference of the modifier to concentrate in aggregates rather than surface fluorinated groups. A contributor to this preference is steric blocking by the bulky 5 kDa PDMS side chains, which works against optimum semifluorinated group intramolecular and intermolecular interactions at the surface. On the other hand, micelles / aggregates are sterically stabilized by a corona of PDMS in the manner similar to conventional amphiphiles.[22] Thus, rigid fluorous side chain self-aggregation in a three dimensional aggregate is preferred relative to a two dimensional surface array.

NIH-PA Author Manuscript

NIH-PA Author Manuscript

NIH-PA Author Manuscript

Depletion of surface D5-3 accounts for the sharp decrease in isopropanol θ_{adv} at and above the CMC. The model shown in Figure 8 explains why "more fluorinated content makes it less oleophobic". This result is interesting because conventional wisdom for increasing oleophobicity is increasing the fluorinated content.[13]

SEM

From the DLS study and the phase diagram in Figure 7, aggregates formed in the two phase region as a function of temperature and composition. The coating process involved dip coating at near ambient conditions under dynamic reaction conditions. The coated slides were placed back under the heat source at 60 °C. At this stage and after final cure at 100 °C the coatings were optically transparent. The model in Figure 8 used to explain wetting behavior requires that aggregates formed during dip coating at ambient temperature do not re-dissolve when the coating was placed under the heat source for initial cure. SEM and TM-AFM were employed to image fracture surfaces of D5-3 modified coatings to find evidence for the presence of aggregates.

Coatings were crosslinked with different concentrations of surface modifier (0, 0.1, 0.3, 1, and 5 wt%) and cured at different temperatures (65, 40, 22, and 0 °C). Condensation cured PDMS plaques have little strength and are easily and smoothly fractured by bending. SEM fracture surface images for three D5-3 modified PDMS samples (0.3, 1, and 5 wt%) cured at 40 °C are shown in Figure 9. Table 2 summarizes observations for all D5-3 modified PDMS samples. A complete set of SEM fracture images corresponding to the observations in Table 2 is provided in Supplemental Information (Figure S6 – S10).

Most of the fractured surfaces have a characteristic rippled structure independent of D5-3 content (Figure 9). In addition, pit-like features are seen in samples with high D5-3 wt% and/or low curing temperatures. Figure 9 shows SEM images for PDMS cured at 40 °C with 5, 1, and 0.3 wt% D5-3. Some of the pit-like features are circled for easy recognition. Table 2 provides a descriptive summary of SEM observations. With increasing D5-3 concentration from 0.3 wt% to 5 wt%, the number and size of the pits increases. Pits were not observed for D5-3 concentrations lower than 0.1 wt%, or for 0.3 wt% compositions cured at higher temperatures. From Table 2, the absence of pits at 0.3 wt% and 23 °C cure is consistent with the D5-3 / PDMS phase diagram for D5-3 concentrations lower than the CMC. Considering the fact that pits are difficult to observe at low concentrations due to the rippled background, these observations are in agreement with DLS that showed no aggregation for a D5-3 concentration of 0.3 wt% at temperatures lower than 23 °C.

The actual feature size determined by SEM (0.5 – 2 μm) is at least an order of magnitude larger than that determined by DLS (10 – 100 nm). DLS measures the hydrodynamic diameter based on differences in refractive indices of particles and solvent, as well as the overall size of the structures. For the acrylate copolymer, the main chain and the fluorinated side chains have different refractive indexes from the silicone solvent, while the silicone side chains have the same refractive index. Thus the main chain and fluorinated side chains that are much smaller than the silicone shell are the principle contributors to light scattering. But the extended silicone side chains in PDMS solvent are the principle contributors to the hydrodynamic diameter due to the slow diffusion rate of aggregates. However, the core-shell structure and possible decoupling of individual D5-3 molecules lead to an apparent particle size that is less than the actual hydrodynamic diameter of the whole aggregate structure. On the other hand, the silicone side chains that are miscible but not chemically reacted with the matrix contribute fully to aggregate size imaged by SEM. Furthermore, the longer time scale of the condensation-curing process may allow larger aggregates form at least during the initial stage when the degree of crosslinking is still low.

NIH-PA Author Manuscript

NIH-PA Author Manuscript

NIH-PA Author Manuscript

In summary, the SEM images account for the presence of D5-3 phase separated aggregates in the PDMS elastomer matrix. As expected based on the model in Figure 8, the number density of the phase separated aggregates increases with increasing D5-3 concentration.

TM-AFM

Fracture surfaces were investigated by TM-AFM so as to better understand the relationship of bulk morphology and D5-3 phase separation described by the model. Figures 10A and 10C show 3D height images for fracture surfaces at 5 and 1 wt% D5-3, respectively. As expected from SEM imaging, 0.3 – 2 μm pits and peaks are observed in proportion to the concentration of D5-3 modifier. These features correspond to aggregates formed by concentrations of D5-3 above the CMC in the crosslinked PDMS matrix.

In the 20 μm × 20 μm phase image for 1 wt% D5-3, only 7 peaks/pits are observed (Figure S11). The number of these features in the 5 wt% D5-3 is about 36 (Figure S12), which is ~ 5 times that for 1 wt%. The asymmetric shape of the pit/peak features in the 3D height images reflects the distortion of the aggregate on fracture. Some of the peaks are close to pits suggesting that the aggregate was pulled apart leaving a residual component adjacent to the pit. To clarify which features are pits and which are peaks, inverted images (Figures 10B and 10D) were obtained. Inspection of these images shows that pits in normal imaging become peaks in inverted images and *vice versa*. The complementarity of the normal and inverted images emphasizes the common origin of pits and peaks.

Conclusions

Surface modification employed by us[10,13] and others[11,12] has generally assumed that increasing the semifluorinated component concentration decreases surface tension, paralleling the asymptotic approach to lower surface tensions commonly found for surfactants in water.[19–21] Wetting behavior for D5-3 modified PDMS coatings provides evidence for a model that is a departure from this notion. Instead, the minimum in surface tension, which corresponds to the maximum θ_{adv} for isopropanol (90°) occurs at the CMC followed by a sharp decline in θ_{adv} at higher concentrations.

Aggregate formation (Figure 8B–C) with concomitant surface depletion provides a model for the sharp transition from predominately molecular species to aggregates at the CMC. The model shown in Figure 8A–C depicts increasing aggregate / micelle concentration with increased D5-3 concentration. A combination of DLS for D5-3 / silicone and morphological imaging of aggregates “trapped” in the coating supports the model in Figure 8 for “more is less”. The result makes plain the stability of micelles or aggregates versus the surface concentrated amphiphile under the dynamic conditions employed for coating preparation. Micelle formation and surface depletion of D5-3 attest to antipodean behavior stemming from fluorous and silicone side chains with radically differing solubility characteristics.

To our knowledge, this is the first time that a marked decrease surface free energy with increasing surface modifier concentration has been observed. One instance of prior research similar to “more is less” comes from surface tension data for **3**, Triton X-100 in formamide.[21] Surface tension versus concentration reported in Figure 1 of the cited reference shows a gradual increase in surface tension above the CMC to a value ~10% higher than the minimum. It is possible that molecular surfactant depletion occurs above CMC for **3** / formamide in a manner similar to “more is less” for D5-3 / PDMS. However, the effect is modest compared to D5-3 / PDMS.

NIH-PA Author Manuscript

NIH-PA Author Manuscript

NIH-PA Author Manuscript

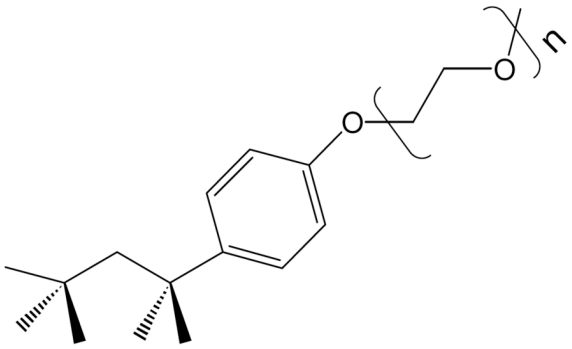

3

Also related is an interesting example of “more is less” from a study of adsorption of oleate on CaF_2 (fluorite) by Mielczarski.[23] High adsorption and buildup of oleate layers on fluorite occurs at $<10^{-4}$ M, but competing processes described in Figure 10 of the cited reference result in greatly diminished oleate adsorption at higher concentrations. Surface depletion of oleate results from thermodynamically favorable formation of oleate species in solution, including micelles. Thus, “more is less” in terms of fluorite-adsorbed oleate.

DCA water $\theta_{adv}/\theta_{rec}$ values for PDMS having D5-3 concentrations less than 2 wt% are cycle dependent and preclude straightforward analysis. Despite the complex cycle-dependent DCA contact angle data for water, an interesting result emerged. D5-3 modification blocked diffusion of low molecular weight PDMS species that usually contaminate water during DCA analysis.

While fluorous polymers like D5-3 with long fluorous side chains have high resistance to water and oil, these polymers can degrade to perfluorooctanoic acid (PFOA) which is bioaccumulative.[24] Future work is aimed at exploring surface modification with short fluorocarbon side chains that form ordered phases.25 This research will be guided by consideration of the novel results using D5-3.

Supplementary Material

Refer to Web version on PubMed Central for supplementary material.

Acknowledgments

The authors thank the National Science Foundation (grants DMR-0207560 and 0802452) and the Office of Naval Research (Contract N00014-08-1-0922) for support of this research. Scanning electron microscopy was performed at the VCU Department of Neurobiology and Anatomy Microscopy Facility supported with funding from NIH-NCRR shared instrumentation grant 1S10RR022495, and in part NIH-NINDS Center core grant 5P30NS047463. The authors also thank the EU for partial financial support through the Framework 6 Integrated Project ‘AMBIO’ (Advanced Nanostructured Surfaces for the Control of Biofouling).

References

1. Lee JN, Park C, Whitesides GM. Analytical Chemistry 2003;75:6544–6554. [PubMed: 14640726]
2. Scheirs, J. Modern Fluoropolymers. West Sussex, England: John Wiley and Sons Ltd.; 1997.
3. Razzano JS. U. S. 7361722. 2008
4. Kobayashi H, Owen MJ. Makromolekulare Chemie-Macromolecular Chemistry and Physics 1993;194:1785–1792.
5. Thanawala SK, Chaudhury MK. Langmuir 2000;16:1256–1260.

NIH-PA Author Manuscript

NIH-PA Author Manuscript

NIH-PA Author Manuscript

6. Maltezos G, Garcia E, Hanrahan G, Gomez FA, Vyawhare S, van Dam RM, Chen Y, Scherer A. Lab on a Chip 2007;7:1209–1211. [PubMed: 17713623]
7. Rolland JP, Van Dam RM, Schorzman DA, Quake SR, DeSimone JM. Journal of the American Chemical Society 2004;126:2322–2323. [PubMed: 14982433]
8. Bullock S, Johnston EE, Willson T, Gatenholm P, Wynne KJ. Journal of Colloid and Interface Science 1999;210:18–36. [PubMed: 9924104]
9. Berglin M, Wynne KJ, Gatenholm P. Journal of Colloid and Interface Science 2003;257:383–391. [PubMed: 16256494]
10. Bertolucci M, Galli G, Chiellini E, Wynne KJ. Macromolecules 2004;37:3666–3672.
11. Iyengar DR, Perutz SM, Dai CA, Ober CK, Kramer EJ. Macromolecules 1996;29:1229–1234.
12. Kim YS, Lee JS, Ji Q, McGrath JE. Polymer 2002;43:7161–7170.
13. Marabotti I, Morelli A, Orsini LM, Martinelli E, Galli G, Chiellini E, Lien EM, Pettitt ME, Callow ME, Callow JA, Conlan SL, Mutton RJ, Clare AS, Kocijan A, Donik C, Jenko M. Biofouling 2009;25:481–493. [PubMed: 19373571]
14. Arrighi V, Gagliardi S, Zhang C, Ganazzoli F, Higgins JS, Ocone R, Telling MTF. Macromolecules 2003;36:8738–8748.
15. Uilk JM, Mera AE, Fox RB, Wynne KJ. Macromolecules 2003;36:3689–3694.
16. Nagy M, Szollosi L, Keki S, Zsuga M. Langmuir 2007;23:1014–1017. [PubMed: 17241007]
17. Katano Y, Tomono H, Nakajima T. Macromolecules 1994;27:2342–2344.
18. Wang JG, Mao GP, Ober CK, Kramer EJ. Macromolecules 1997;30:1906–1914.
19. Weschayanwiwat P, Scamehorn JF, Reilly PJ. Journal of Surfactants and Detergents 2005;8:65–72.
20. Li GL, Zheng LQ, Xiao JX. Journal of Fluorine Chemistry 2009;130:674–681.
21. Das J, Ismail K. Journal of Colloid and Interface Science 2009;337:227–233. [PubMed: 19540507]
22. Chern CS, Liou YC. Polymer 1999;40:3763–3772.
23. Mielczarski JA, Mielczarski E, Cases JM. Langmuir 1999;15:500–508.
24. Harada K, Koizumi A, Saito N, Inoue K, Yoshinaga T, Date C, Fujii S, Hachiya N, Hirosawa I, Koda S, Kusaka Y, Murata K, Omae K, Shimbo S, Takenaka K, Takeshita T, Todoriki H, Wada Y, Watanabe T, Ikeda M. Chemosphere 2007;66:293–301. [PubMed: 16793116]
25. Zheng Y, Wynne KJ. Langmuir 2007;23:11964–11967. [PubMed: 17958389]

NIH-PA Author Manuscript
NIH-PA Author Manuscript
NIH-PA Author Manuscript

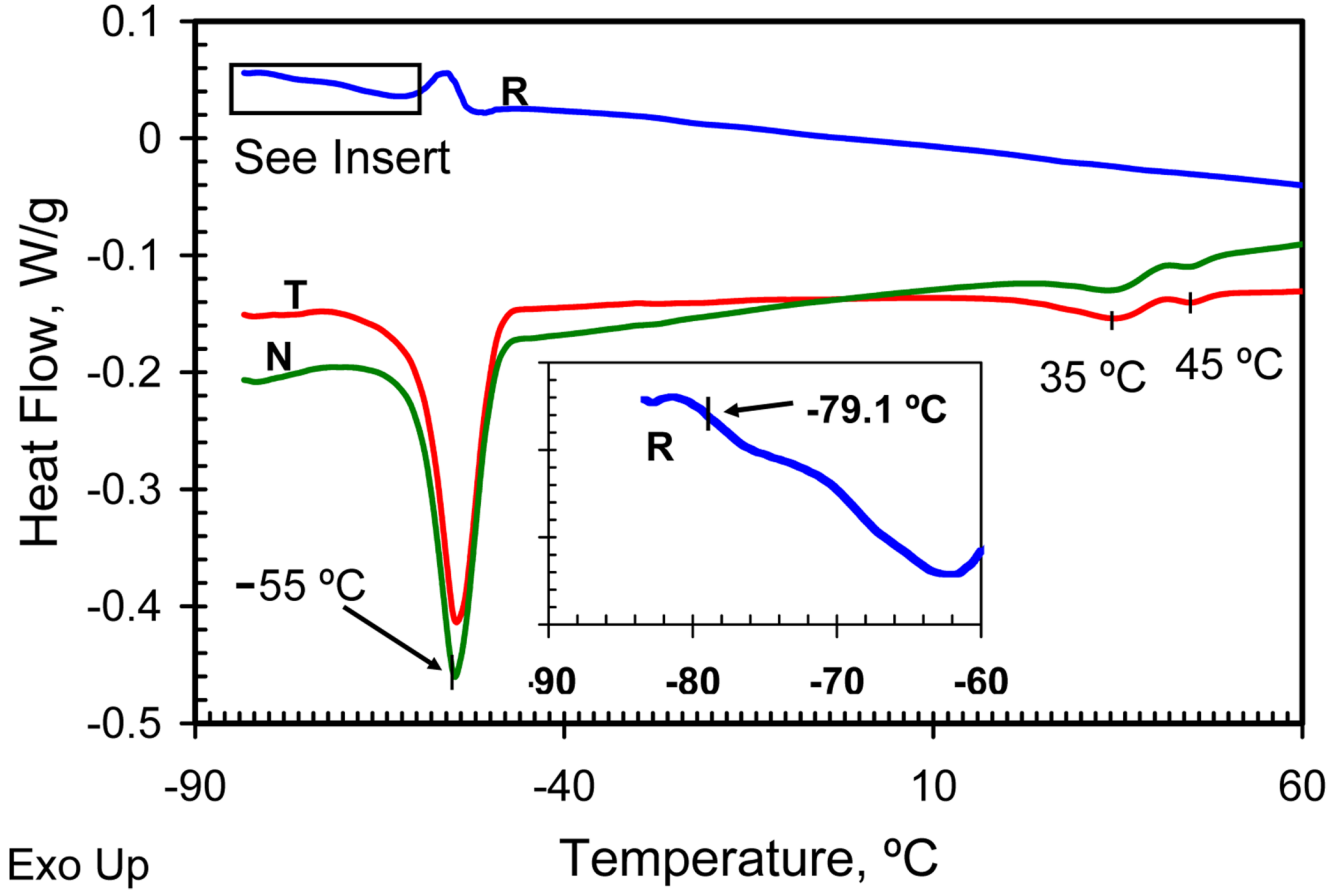

Figure 1.
Thermal transitions of copolymer D5-3 by modulated DSC. **T** (red), total heat flow; **R** (insert, blue), reversing heat flow; **N** (green), non-reversing heat flow.

NIH-PA Author Manuscript
NIH-PA Author Manuscript
NIH-PA Author Manuscript

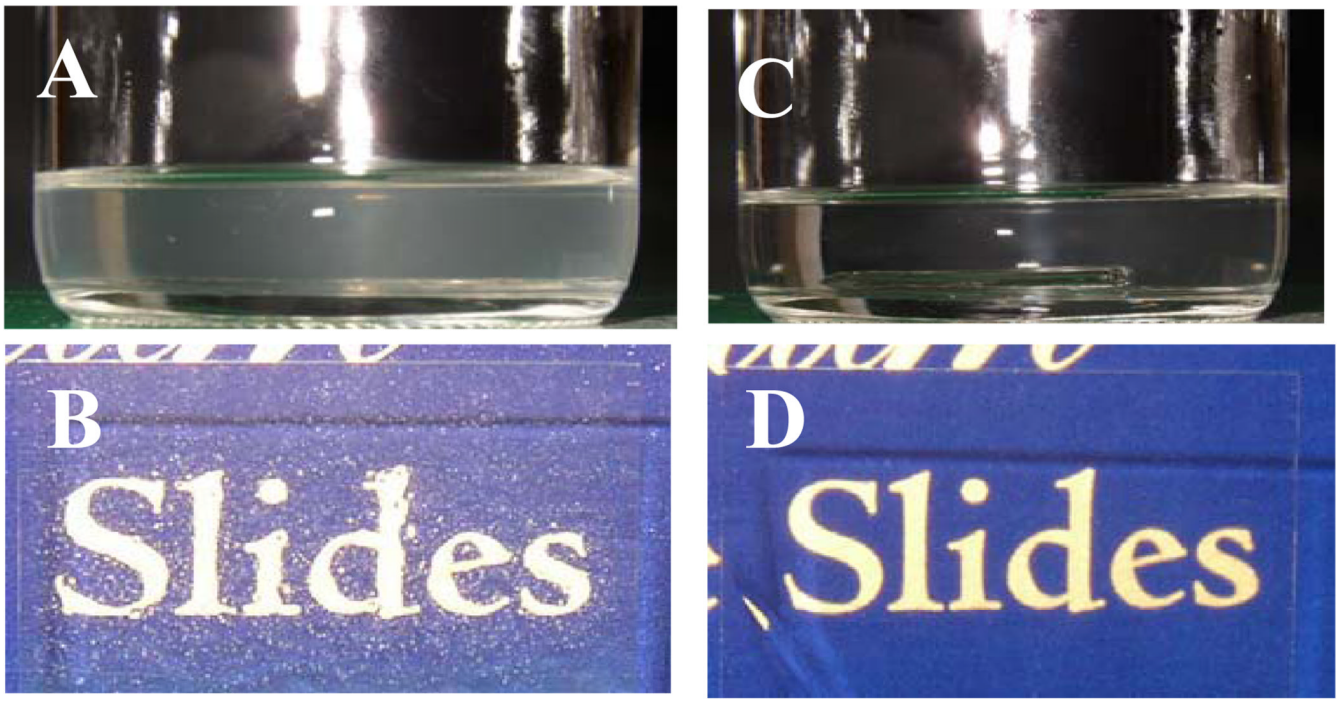

Figure 2.
The appearance of 2 wt% D5-3/PDMS solutions and coated slides prepared without (**A**, **B** left) and with (**C**, **D** right) heating to 60–65 °C via an infrared lamp.

NIH-PA Author Manuscript

NIH-PA Author Manuscript

NIH-PA Author Manuscript

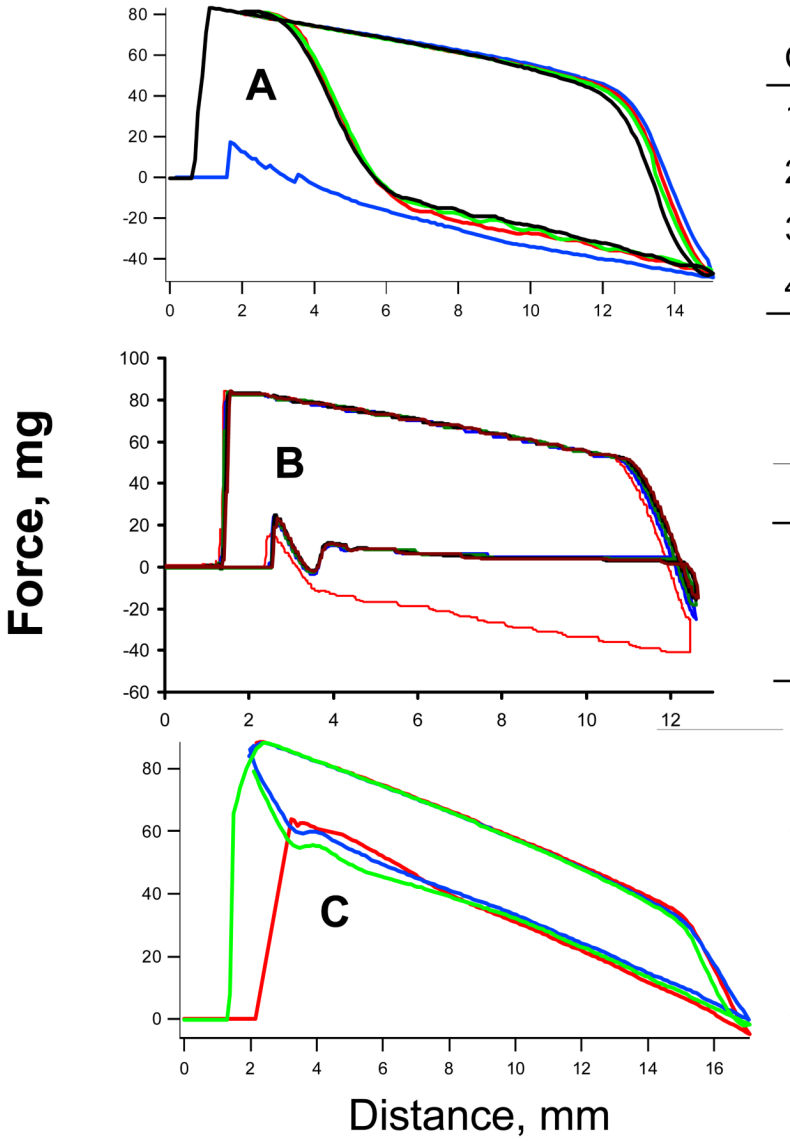

Cycle	θ_{adv}	θ_{rec}
1, red	89	33
2, blue	90	33
3, green	86	33
4, black	85	33

Cycle	θ_{adv}	θ_{rec}
1, red	94	29
2-5 (superposed)	84	29

Cycle	θ_{adv}	θ_{rec}
1, red	46	23
2, blue	47	23
3, green	47	23

Figure 3.
DCA force distance curves (isopropanol) for **A**, D5-3 (neat), **B**, 0.4 wt% D5-3/PDMS **C**, 2 wt % D5-3/PDMS.

NIH-PA Author Manuscript
NIH-PA Author Manuscript
NIH-PA Author Manuscript

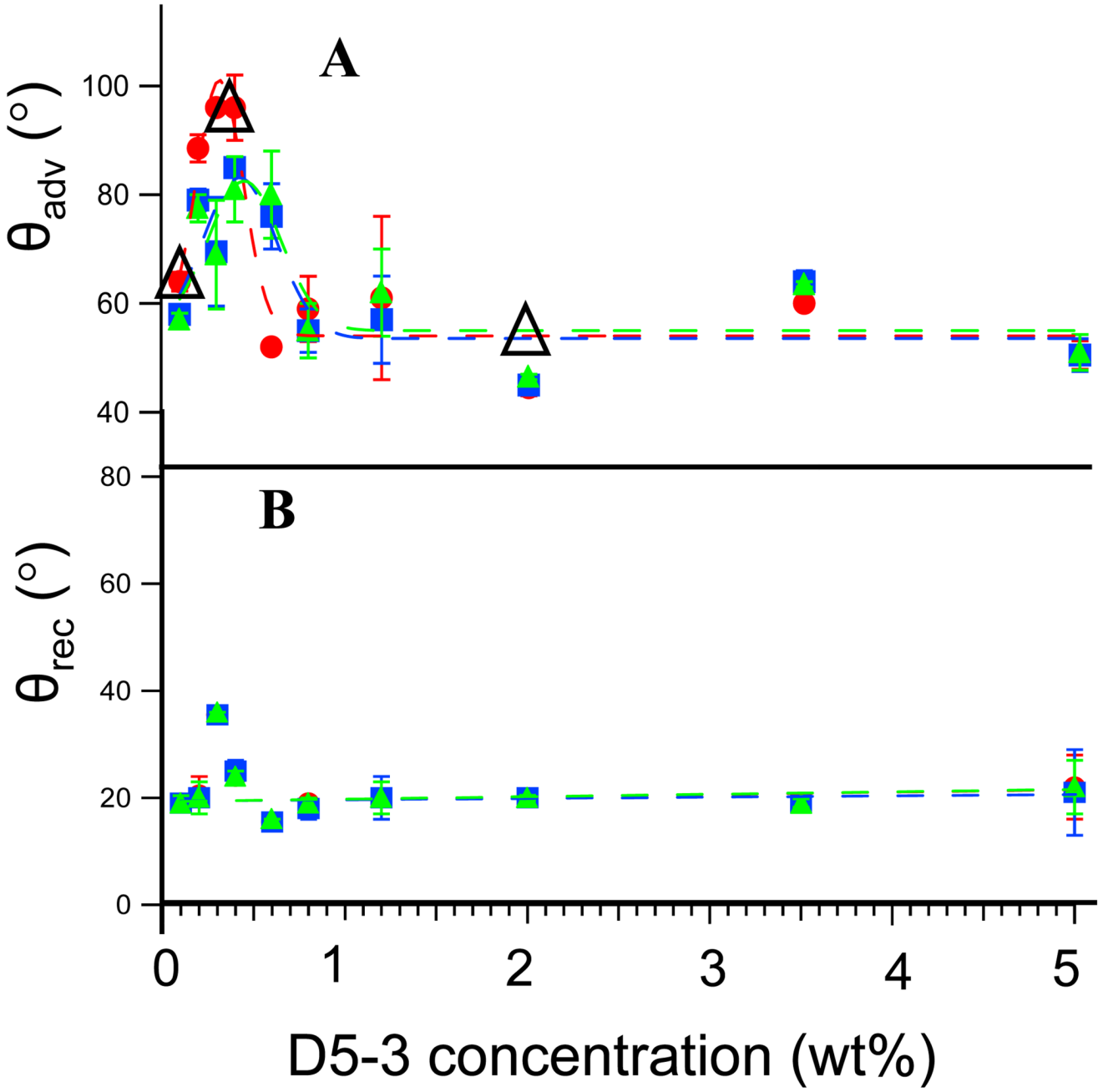

Figure 4.
Isopropanol dynamic contact angles (**A**, θ_{adv}) and (**B**, θ_{rec}) for condensation cured 26 kDa PDMS as a function of increasing weight percent of D5-3 surface modifier: ●, 1st cycle; ■, 2nd cycle; ▲, 3rd cycle. Points represented by Δ are duplicate determinations taken with a new batch of materials.

NIH-PA Author Manuscript

NIH-PA Author Manuscript

NIH-PA Author Manuscript

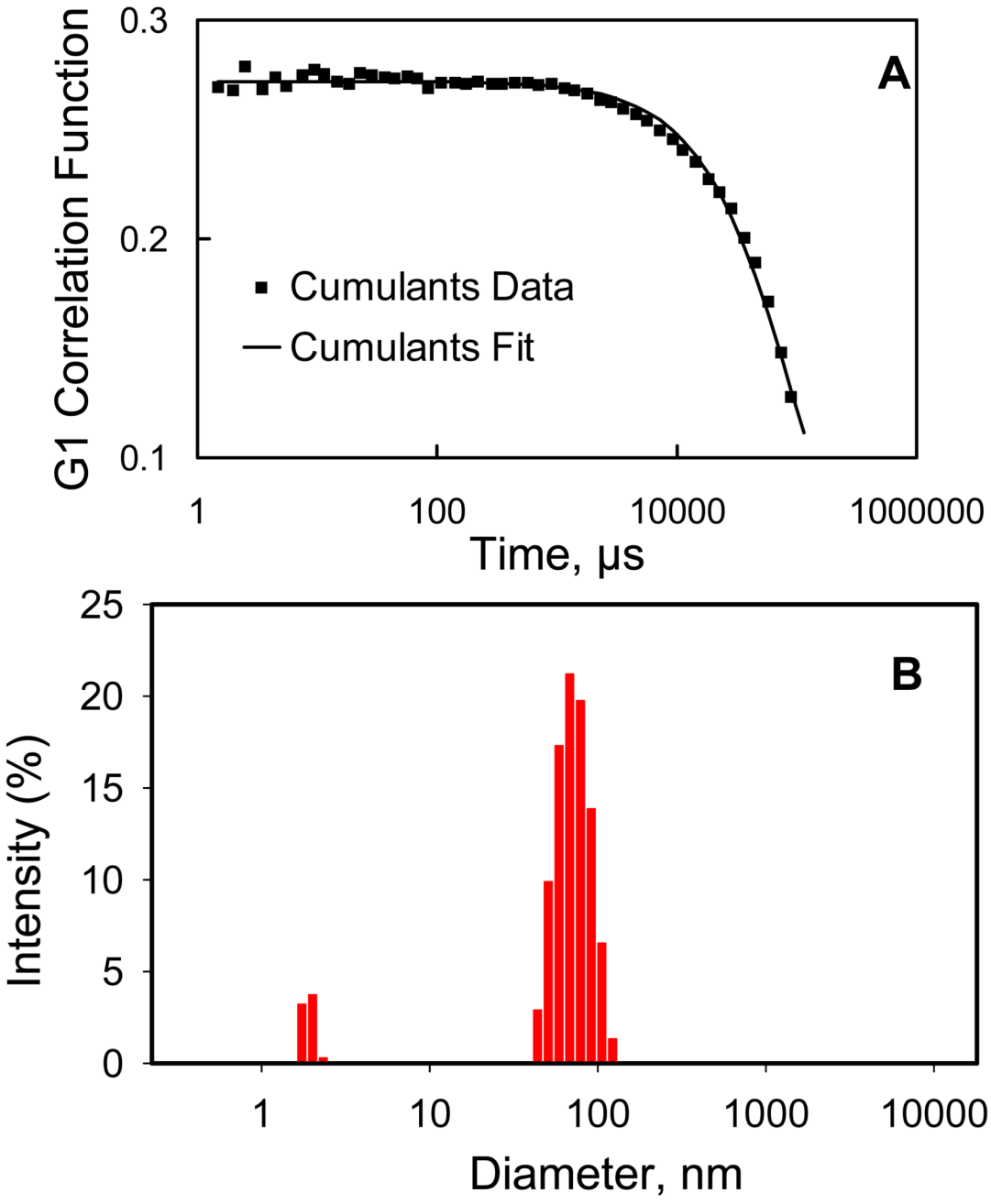

Figure 5.

DLS data for 1 of 16 measurements on 3 wt% D5-3 in PDMS at 20 °C: **A**, Correlation function (data points) and cumulant analysis (solid line); fitting of the correlation function used the "multiple narrow size distribution" setting; **B**, histograms for particle diameters.

NIH-PA Author Manuscript
NIH-PA Author Manuscript
NIH-PA Author Manuscript

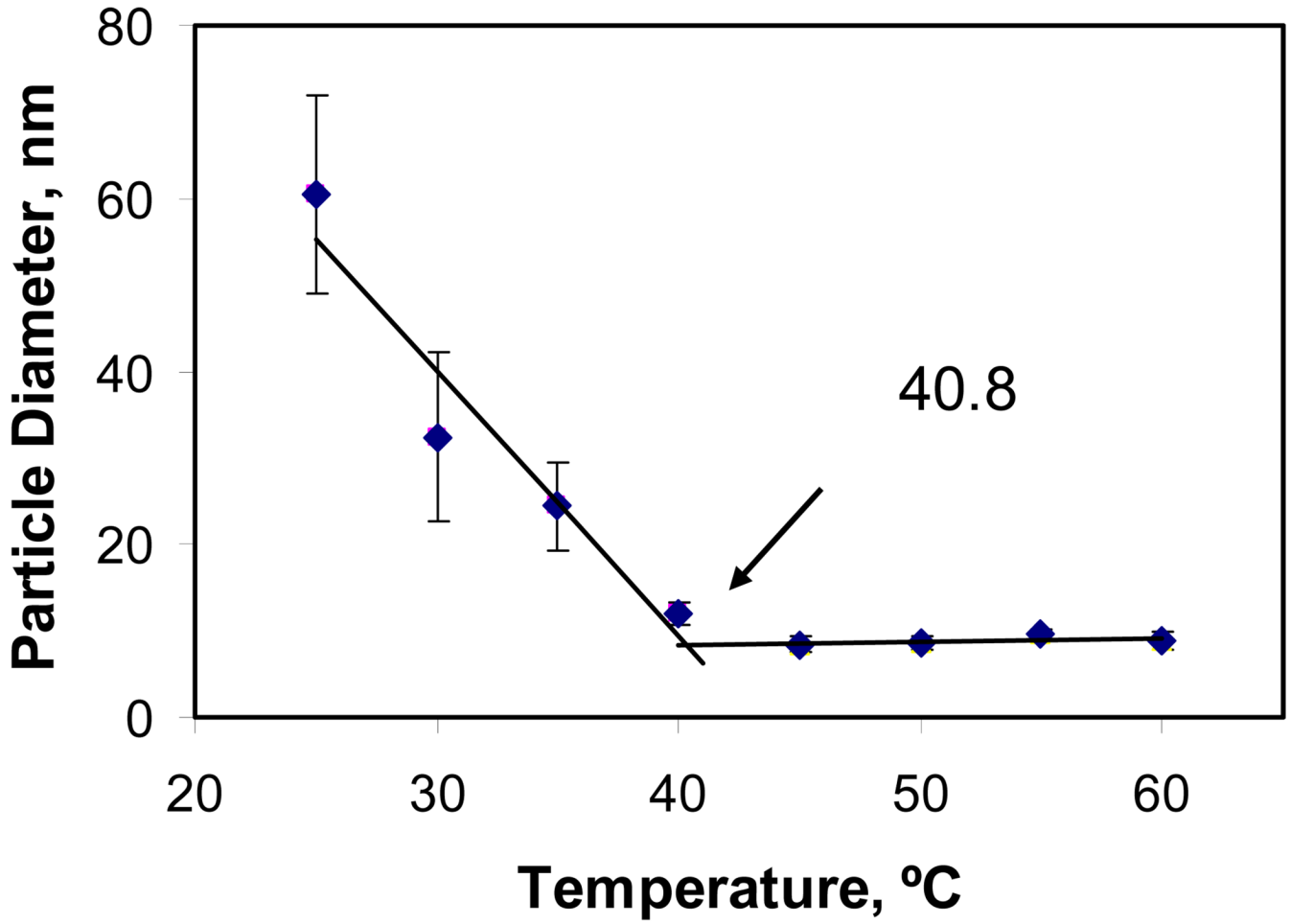

Figure 6.
Particle diameter vs. temperature for 5 wt% D5-3 in PDMS.

NIH-PA Author Manuscript

NIH-PA Author Manuscript

NIH-PA Author Manuscript

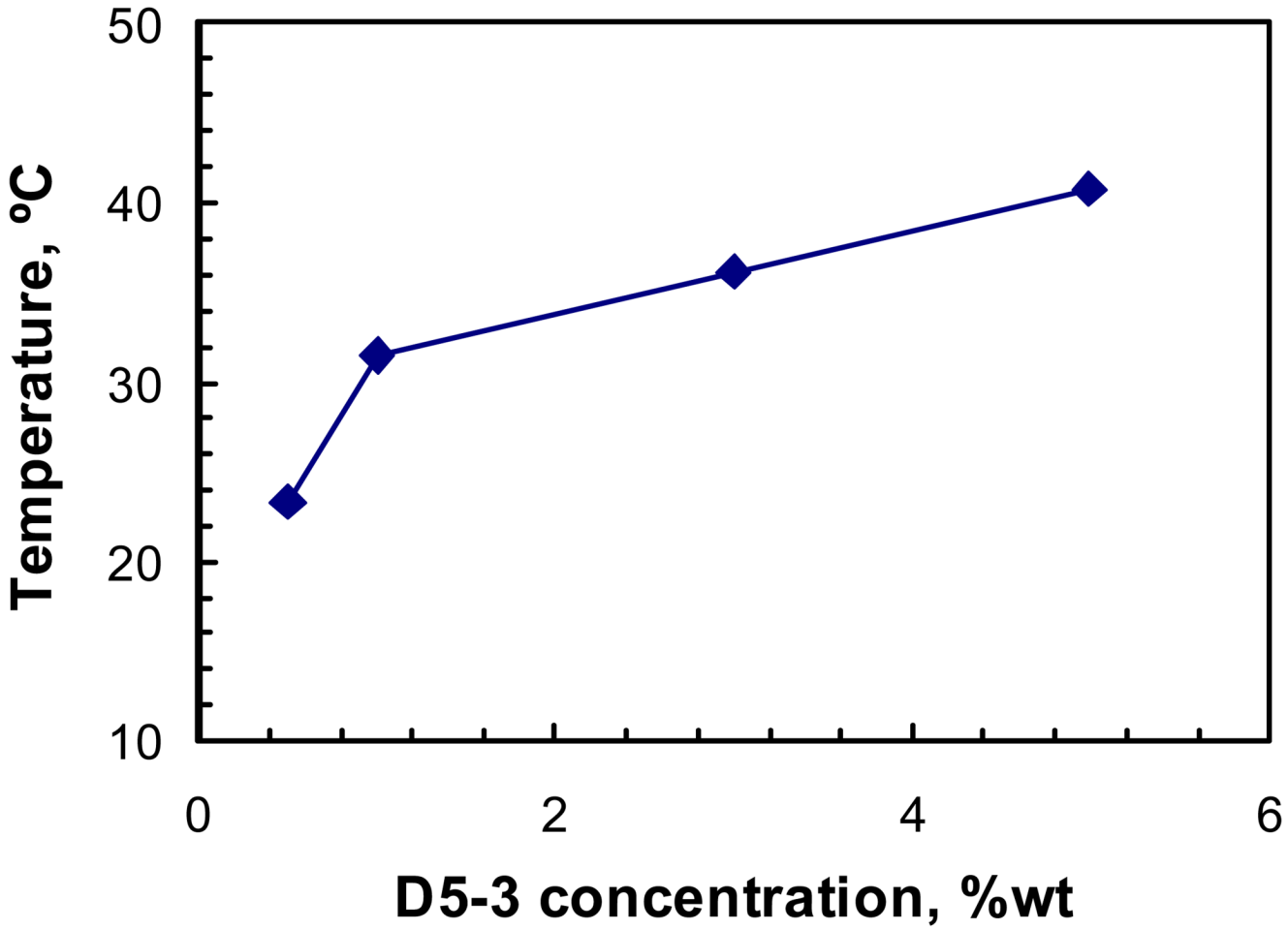

Figure 7.
Phase diagram showing temperature vs. D5-3 composition at the CMC.

NIH-PA Author Manuscript
NIH-PA Author Manuscript
NIH-PA Author Manuscript

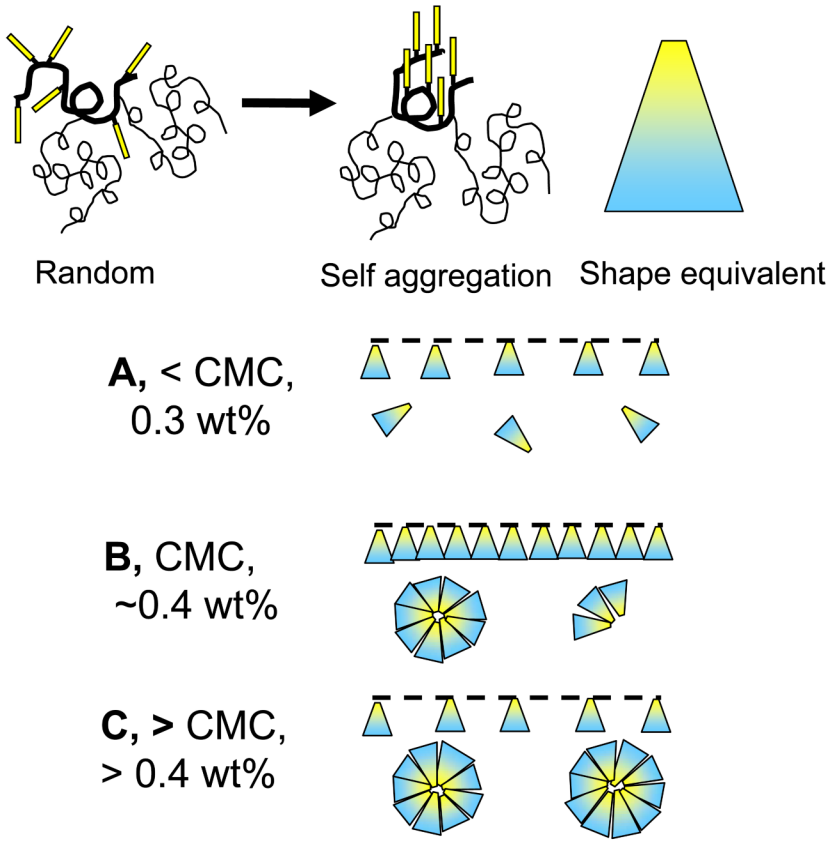

Figure 8.

Top: Proposed initial stage for self aggregation of D5-3. The result is depicted as a cone-like shape which is represented in two dimensions as a trapezoid. The blue end is PDMS; the yellow end is the self-aggregated semifluorinated groups. **Bottom**: Three regimes for proposed self-aggregation of D5-3. **A**, rapid buildup of semifluorinated surface concentration in dilute solution; **B**, maximum semifluorinated surface concentration near the CMC; **C**, D5-3 surface-depletion above the CMC.

NIH-PA Author Manuscript
NIH-PA Author Manuscript
NIH-PA Author Manuscript

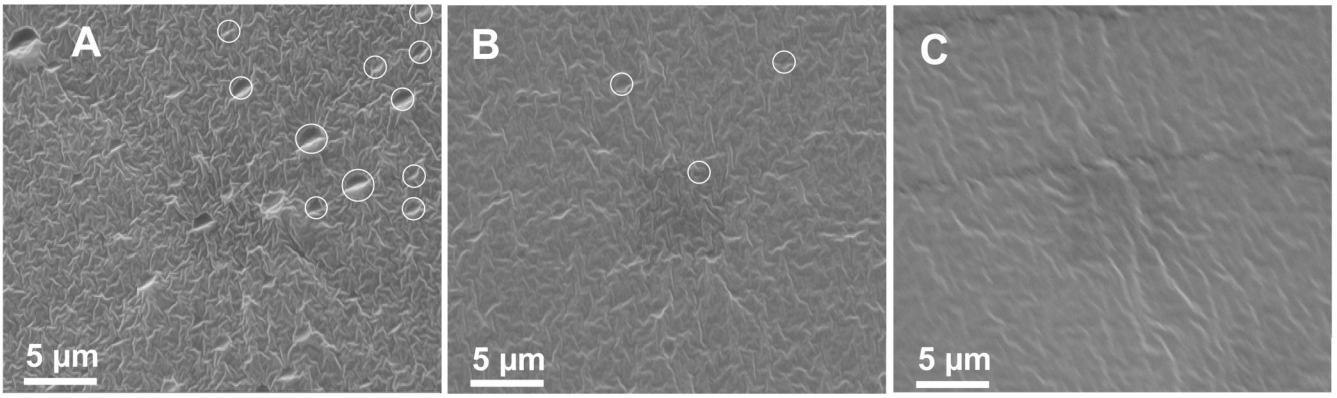

Figure 9.
SEM images for the fracture surface of condensation cured (40 °C) PDMS containing: **A**, 5; **B**, 1, and **C**, 0.3 wt% D5-3.

NIH-PA Author Manuscript
NIH-PA Author Manuscript
NIH-PA Author Manuscript

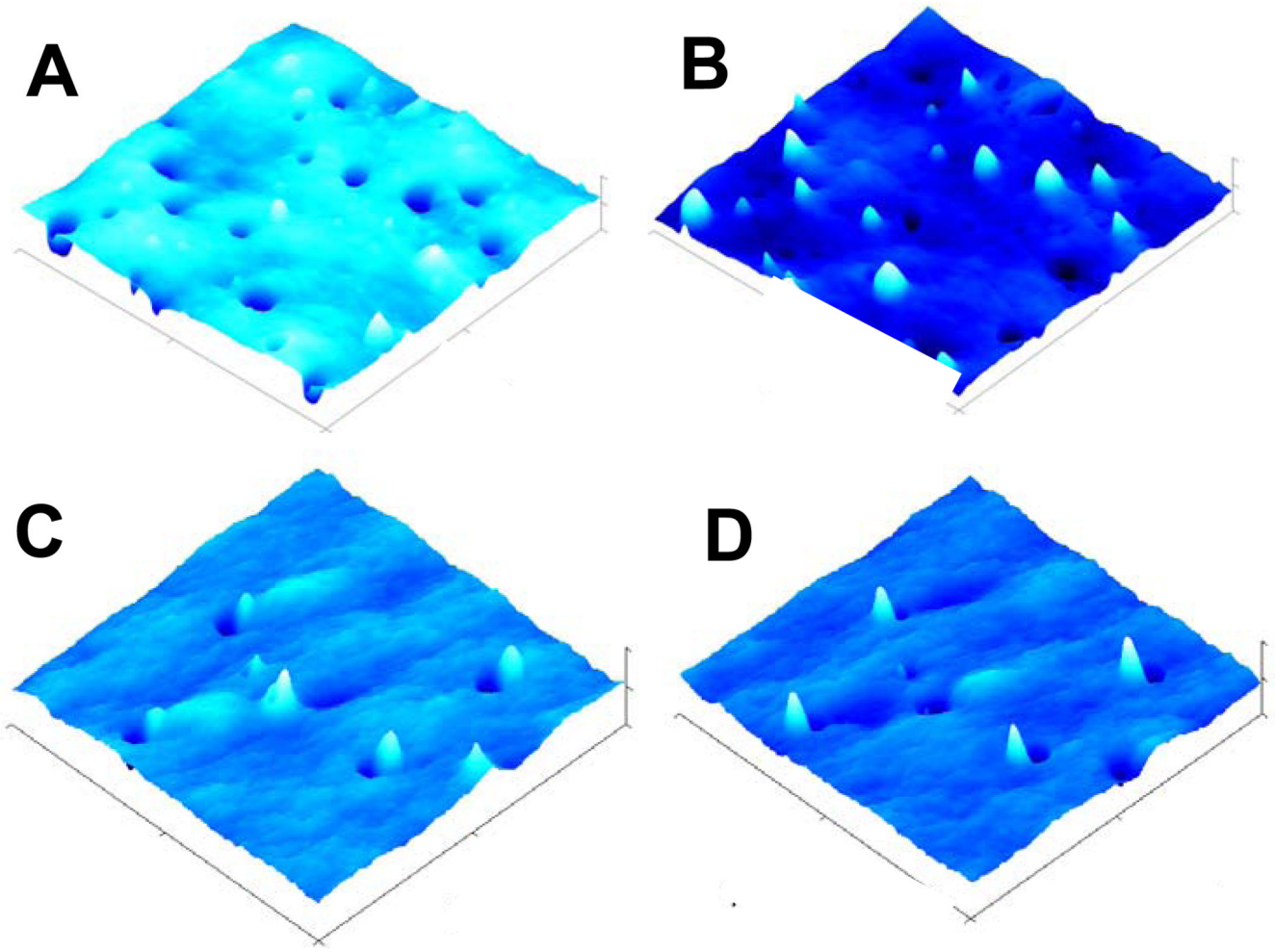

Figure 10.
TM-AFM 3D-images (20 × 20 μm) for 5 wt% (**A**, **B**) and 1 wt% (**C**, **D**) D5-3 PDMS modified coatings. **B** and **D** are inverted images; z range, **A**, **B**, 1300 nm; **C**, **D**, 500 nm; $A/A_o = r_{sp}$ = setpoint ratio = 0.80; R_q (**A**) = 104 nm; R_q (**B**) = 25 nm.

NIH-PA Author Manuscript
NIH-PA Author Manuscript
NIH-PA Author Manuscript

Langmuir. Author manuscript; available in PMC 2011 April 20.

Table 1

DLS results for PSM D5-3 in PDMS. Mean particle diameter (z-average) of aggregates measured by Dynamic Light Scattering (nm).[a,b]

Concentration, wt%	Temperature, °C										
	10	**15**	**20**	**25**	**30**	**35**	**40**	**45**	**50**	**55**	**60**
0	nd	nd	nd	nd	nd	nd	nd	n	nd	n	nd
0.1	nd	nd	nd	nd	nd	nd	nd	n	nd	n	nd
0.3	nd	nd	nd	nd	nd	nd	nd	n	nd	n	nd
0.5	n	**30±10**	**24±12**	**13±4**	**12±4**	n	13±3	10±1	n	n	10±2
1	n	n	**53±13**	**22±4**	**20±3**	11±1	11±2	n	9±1	n	11±2
3	n	n	**42±15**	**33±11**	**17±2**	**17±3**	12±1	11±1	11±1	n	11±1
5	n	n	n	**61±12**	**34±10**	**27±6**	**14±1**	10±1	11±1	13±1	13±2

[a] n, no measurement; nd, measurement was performed, but micelle formation was not detected.

[b] The sizes are in the form of the z-average diameter (nm), as derived from DLS measurements. For each determination, 10–20 measurements were performed and the average and standard deviation are reported.

NIH-PA Author Manuscript

NIH-PA Author Manuscript

NIH-PA Author Manuscript

Table 2

SEM features for fracture surfaces of condensation-cured silicones modified with D5-3..

Temp→ Composition (wt%)↓	**65 °C**	**40 °C**	**22 °C**	**0 °C**
5	Large holes (6/100 μm^2)	Mixed size holes (8/100 μm^2) and ripples	Mixed size holes (8/100 μm^2) and ripples	Mixed size holes (10/100 μm^2) and ripples
1	Mixed size holes (1/100 μm^2) and ripples	Small holes (3/100 μm^2) and ripples	Small holes (3/100 μm^2) and ripples	Small Holes (4/100 μm^2) and ripples
0.3	Ripples	Ripples	Very small holes (2/100 μm^2) and ripples	Very small holes (2/100 μm^2) and ripples
0.1	Ripples	Ripples	Ripples	Ripples
0	None	Ripples	Ripples	Ripples